Synthesis and Structures of High-Quality Single-Crystalline II3-V2 Semiconductors Nanobelts

ARTICLE *in* THE JOURNAL OF PHYSICAL CHEMISTRY C · APRIL 2007

Impact Factor: 4.77 · DOI: 10.1021/jp068792s

3 AUTHORS, INCLUDING:

Guozhen Shen
Chinese Academy of Sciences
217 PUBLICATIONS **7,266** CITATIONS
SEE PROFILE

Dmitri Golberg
National Institute for Materials Science
646 PUBLICATIONS **22,786** CITATIONS
SEE PROFILE

Synthesis and Structures of High-Quality Single-Crystalline II_3-V_2 Semiconductors Nanobelts

Guozhen Shen,* Yoshio Bando, and Dmitri Golberg

Nanoscale Materials Center, National Institute for Materials Science (NIMS), Namiki 1-1, Tsukuba, Ibaraki 305-0044, Japan

Received: December 21, 2006; In Final Form: February 4, 2007

Due to the difficulties, such as lack of generalized synthetic methodologies, production of amorphous materials, diffraction pattern problems, and instability in air, etc., associated with II_3-V_2 semiconducting compounds (II and V indicate elements of Group II and Group V.), single-crystalline II_3-V_2 nanostructures are intrinsically harder to prepare and it has been a great challenge to produce single-crystalline one-dimensional II_3-V_2 nanostructures. Here, by using a mixture of ZnS (or CdS) and Mn_3P_2 as the source materials, we demonstrate the successful synthesis of high-quality single-crystalline Zn_3P_2 and Cd_3P_2 nanobelts. Systematic structural analyses, such as X-ray diffraction, scanning electron microscopy, high-resolution transmission electron microscopy, and energy dispersive spectrometer, were performed on these novel II_3-V_2 nanomaterials. By a judicious choice of source materials, II_3-V_2 nanobelts with compositions other than Cd_3P_2 and Zn_3P_2, such as Cd_3As_2, Zn_3As_2, etc., may also be fabricated.

1. Introduction

Rational design and synthesis of nanoscale materials are important with respect to understanding fundamental properties, creating miniaturized devices, and developing nanotechnologies.[1,2] Analysis of one-dimensional (1D) nanostructures, such as nanotubes, nanowires, and nanobelts, might shed light on the role of dimensionality in physical properties. In addition, these novel nanomaterials are expected to play a central role in new revolutionary applications ranging from molecular electronics to scanning probe microscopy probes.[3,4] Many inorganic materials have been found to form 1D nanostructures, such as graphite, metals, II−VI semiconductors, III−V semiconductors, oxides, and many others.[3−15]

Semiconducting II_3-V_2 compounds, with narrow band gaps, are of great scientific and technological importance.[16] Due to the large excitonic radii, they are suggested to exhibit pronounced size quantization effects. Bulk II_3-V_2 compound semiconductors have many potential applications in infrared detectors, lasers, solar cells, ultrasonic multipliers, and Hall generators.[17] However, compared with the significant progress in the studies of 1D nanoscale II−VI and III−V semiconductors, research on nanoscale II_3-V_2 semiconductors has been lingering far behind. Only a handful of papers have been published due to the significant experimental difficulities, such as lack of generalized synthetic methodologies, relative ease in the material amorphization, instability in air, etc. These problems make the preparation of II_3-V_2 compound nanostructures intrinsically difficult. For example, no crystalline XRD data were obtained on quantum dots of Zn_3P_2 and Cd_3P_2 prepared through metal−organic processes.[18,19] The synthesis of 1D II_3-V_2 compound nanostructures, namely, the trumpet-like Zn_3P_2 nanostructures and Zn_3P_2 and Cd_3P_2 nanotubes, was recently accomplished by our group.[20] However, to date, the synthesis of diverse high-quality, single-crystalline 1D II_3-V_2 compound nanostructures still remains a challenge.

In this paper, by using a mixture of ZnS (or CdS) and Mn_3P_2 as the source materials, we demonstrate the successful synthesis of high-quality single-crystalline II_3-V_2 semiconductors, Zn_3P_2 and Cd_3P_2 nanobelts, on a large scale and systematically analyze their structures and crystallography.

2. Experimental Section

Zn_3P_2 and Cd_3P_2 nanobelts were prepared in a vertical high-frequency induction furnace as shown in Scheme 1. The furnace consists of a fused quartz tube and an induction-heated cylinder made of high-purity graphite coated with a carbon fiber thermoinsulating layer and has two inlets on its top and base, respectively, and one outlet on its base. A graphite crucible, containing a mixture of ZnS (or CdS) and Mn_3P_2 with a molar ratio of 1:1.2, was placed at the center cylinder zone. After evacuation of the quartz tube to ~20 Pa, two pure Ar flows were introduced through the inlet at a flow rate of 50 (top) and 250 sccm (base), respectively, creating the ambient pressure in the furnace. The crucible was rapidly heated to 1350 °C in 10 min and maintained at this temperature for 50 min. Then the power generator was switched off allowing the crucible to cool to room temperature naturally. The processing temperature was measured by an optical pyrometer with an estimated accuracy of ±10 °C. After reaction, wool-like products were found deposited on the inner wall of the graphite cylinder where the temperature is about 900 °C.

The structures and morphologies of the products were characterized by using an X-ray powder diffractometer (RINT 2200F) with Cu Kα radiation, a scanning electron microscope (SEM, JSM-6700F), and a field-emission transmission electron microscope (TEM, JEM-3000F) equipped with an energy-dispersive X-ray spectrometer (EDS).

* Address correspondence to this author. E-mail: shen.guozhen@nims.go.jp, gzshen@ustc.edu. Fax: +81-29-8516280.

10.1021/jp068792s CCC: $37.00
Published on Web 03/09/2007

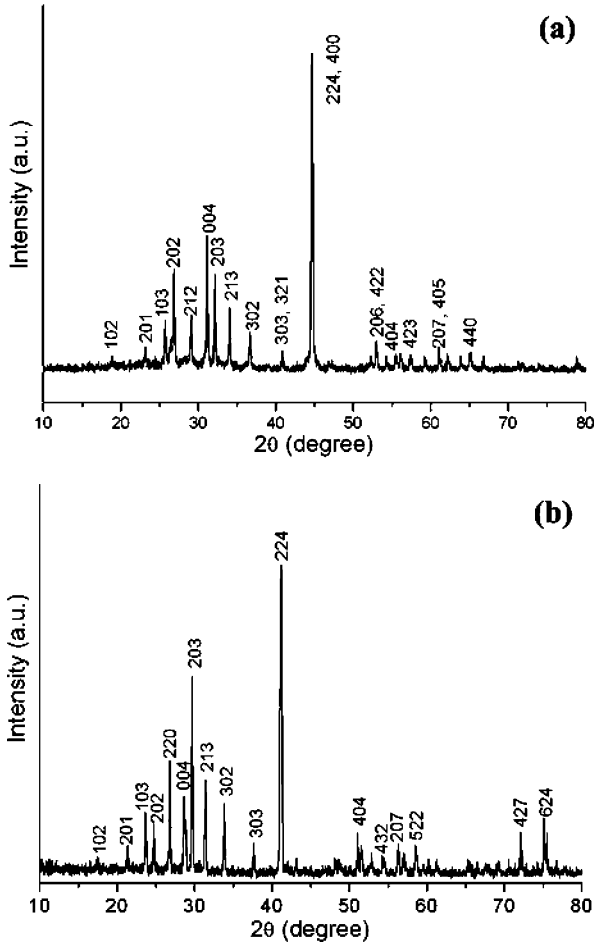

Figure 1. XRD patterns of the synthesized (a) Zn_3P_2 and (b) Cd_3P_2.

SCHEME 1: Schematic Diagram of the Furnace Utilized in the Experiments

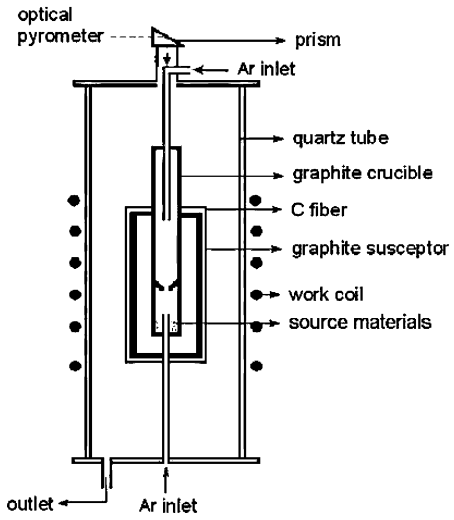

3. Results and Discussion

3.1. Structure. The structures and phase purities of the synthesized products were checked by using XRD. Figure 1 shows the XRD patterns of the deposited products. All X-ray peaks in Figure 1a can be easily indexed to tetragonal Zn_3P_2 phase with cell constants comparable to those reported in the literature (JCPDS file, No. 65-2854). No peaks of other crystalline phases are detected in the pattern, indicating the formation of a pure Zn_3P_2 material. Figure 1b is the XRD pattern of the product synthesized from CdS and Mn_3P_2, which can be indexed to the pure tetragonal Cd_3P_2 phase without other impurities (JCPDS file, No. 65-2856).

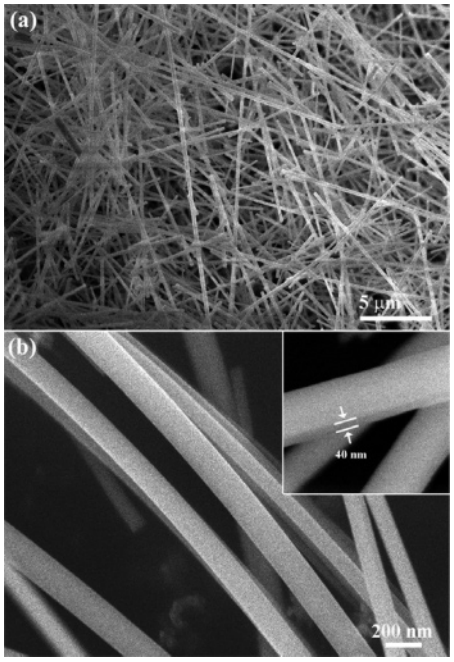

Figure 2. SEM images of the synthesized Zn_3P_2, showing 1D belt-like morphology.

3.2. Zn_3P_2 Nanobelts. The morphology of the synthesized Zn_3P_2 product was first checked by scanning electron miscroscopy (SEM). Figure 2a shows a SEM image of a Zn_3P_2 product, which indicates the formation of 1D nanostructures with lengths ranging from several tens to hundreds of micrometers on a large scale. A high-magnification SEM image shown in Figure 2b reveals that the 1D Zn_3P_2 nanostructures are actually nanobelts with rectangular cross-sections. The nanobelts have diameters of about 100−200 nm and a wall thickness of about 40 nm.

Figure 3a is a TEM image of a single Zn_3P_2 nanobelt with a diameter of 150 nm. The inset is the selected area electron diffraction (SAED) pattern recorded along the $[\bar{1}01]$ zone axis of Zn_3P_2, which indicates that the nanobelt is of single crystalline nature. X-ray energy dispersive spectra (EDS) generated with an electron nanoprobe (∼20 nm) were collected from different spots along the nanobelt. A typical EDS spectrum is shown in Figure 3b, which shows that the nanobelt consists of only Zn and P with an atomic ratio of ∼3:2, indicating the formation of pure Zn_3P_2 structure. This is consistent with the XRD result. The signal of copper in this spectrum comes from the copper grid used for TEM analysis. A HRTEM image of the synthesized Zn_3P_2 nanobelt is demonstrated in Figure 3c. The measured *d* spacings of 0.66 and 0.81 nm perpendicular to and along the longitudinal axis of the nanobelt are in agreement with those of the tetragonal Zn_3P_2 (101) and (010) planes, respectively. A fast Fourier transform (FFT) pattern shown in the inset to Figure 3c is a typical pattern along the $[\bar{1}01]$ zone axis of tetragonal Zn_3P_2. Thus, the growth direction of the Zn_3P_2 nanobelt is determined to be parallel to the [010] crystallographic orientation. The synthesized Zn_3P_2 nanobelts have clean surfaces without any sheathed materials, which is different from the trumpet-like Zn_3P_2 nanowires synthesized with use of GaP and ZnS as the source materials.[20a] In fact, in the present work, extremely high purity Ar gas, high purity source materials are used, which avoid surface oxidization.

3.3. Cd_3P_2 Nanobelts. Figure 4 depicts the SEM images of the synthesized Cd_3P_2 product. It indicates the formation of large

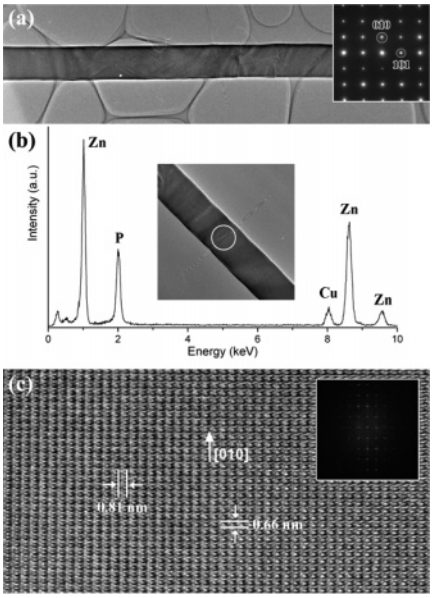

Figure 3. (a) TEM image of an individual Zn_3P_2 nanobelt and its SAED pattern. (b) EDS spectrum taken from a Zn_3P_2 nanobelt. (c) HRTEM image of the part of a Zn_3P_2 nanobelt showing its single crystalline nature and the growth direction along the [010] orientation. Inset: FFT image.

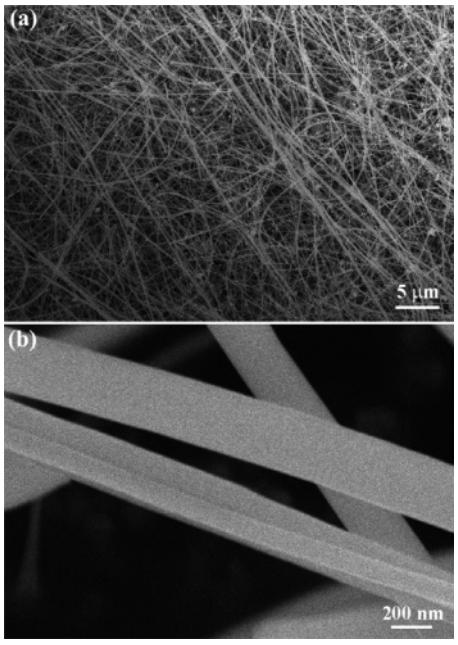

Figure 4. SEM images of the synthesized Cd_3P_2 nanobelts.

scale 1D nanobelts. The nanobelts have diameters of 100−500 nm, thickness of ca. 70 nm, and lengths of hundreds of micrometers.

The TEM image of the synthesized Cd_3P_2 products is shown in Figure 5a. The tips of the Cd_3P_2 nanobelts are flat. No particles were found attached to the tips, indicating that the vapor−liquid−solid (VLS) process may not be the dominant mechanism for the growth of Cd_3P_2 nanobelts. The apparent ripplelike contrast in the image is due to the strain resulting from the belt bending according to previous reports. The belt-shaped structures can also be clearly seen in the TEM image shown in Figure 5b. The twisted belt shows that the thickness was ca. 70 nm. The EDS spectrum (Figure 5c) taken from the part framed in the figure inset confirms that the belt is composed of only Cd and P.

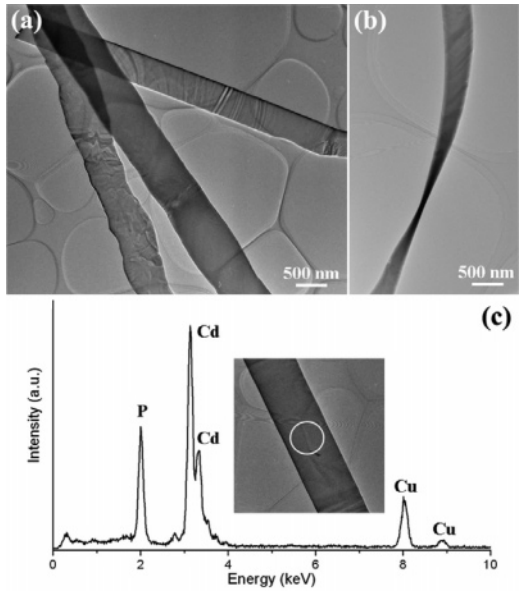

Figure 5. (a) TEM image of the synthesized Cd_3P_2 nanobelts. (b) TEM image of a single Cd_3P_2 nanobelt showing twisted morphology. (c) EDS spectrum taken from one Cd_3P_2 nanobelt.

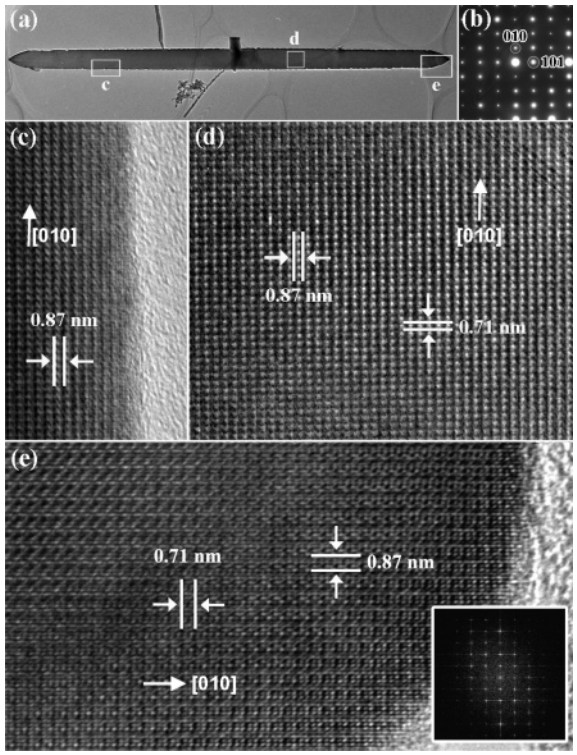

Figure 6. (a) TEM image of a single Cd_3P_2 nanobelt and (b) its SAED pattern. (c−e) HRTEM images taken from the parts framed in part a. These show a single crystalline character and the growth direction along the [010] direction. Inset: FFT image.

Figure 6a is the TEM image of another Cd_3P_2 nanobelt. Its SAED pattern, shown in Figure 6b, is recorded along the $[\bar{1}01]$ zone axis of Cd_3P_2, which indicates the formation of single crystalline nanobelt. Parts c−e of Figure 6 are the corresponding lattice-resolved HRTEM images of the parts framed in Figure 6a, corresponding to the surface, the body, and the tip of the Cd_3P_2 nanobelt, respectively. The clearly resolved lattice fringes perpendicular to and along the longitudinal axis of the nanobelt in all these images are 0.71 and 0.87 nm, respectively, which correspond to the (101) and (010) lattice planes of tetragonal Cd_3P_2. Dozens of nanobelts have been checked and they all

have the same structure. Taking into account the typical FFT pattern shown in the Figure 6e inset, it is concluded that the synthesized Cd_3P_2 nanobelts have the preferred growth directions along the [010] crystallographic orientations.

3.4. Growth Mechanism. The formation of single-crystalline Zn_3P_2 and Cd_3P_2 nanobelts proceeds via a simple thermal reaction process with only ZnS (or CdS) and Mn_3P_2 powders as source materials. Since no catalysts are used in the process and all the tips of the synthesized nanobelts are free of attached particles, the vapor−solid (VS) mechanism[21] can be used to explain the growth process of the nanobelts. At high reaction temperature, ZnS or CdS reacts with C (coming from the graphite crucible) via the reaction $ZnS + C \rightarrow Zn + CS_2$ or $CdS + C \rightarrow Cd + CS_2$ to produce gaseous Zn or Cd.[20] At the same time, Mn_3P_2 also thermally decomposes to generate gaseous P. The produced Zn gaseous (or Cd gaseous) and gaseous P then react with each other via the reaction $3Zn + 2P \rightarrow Zn_3P_2$ or $3Cd + 2P \rightarrow Cd_3P_2$ to generate gaseous Zn_3P_2 or Cd_3P_2, which are transferred to the low-temperature region and deposit on the wall of the crucible and grow longitudinally to form 1D Zn_3P_2 or Cd_3P_2 nanobelts.

The present VS growth model is quite different from the one used to grow II_3-V_2 nanotubes, which are governed by an in situ template model. In this work, two gas flows were introduced into the reaction system at high volumes from both the top and the base of the furnace. The high volume gases warrant the reaction gases generated at high temperature mixed homogeneously and directly reacted with each other to generate gaseous Zn_3P_2 or Cd_3P_2 instead of the first formation of Zn or Cd nanorods and Zn_3P_2 or Cd_3P_2, thus a different growth process occurred.

3.5. Vapor−Liquid−Solid (VLS) Grown II_3-V_2 Nanobelts. The above analyses confirm that II_3-V_2 nanobelts, such as Zn_3P_2 nanobelts and Cd_3P_2 nanobelts, are successfully synthesized via a VS process. In fact, it was found that by using a VLS process, nanobelts of II_3-V_2 can also be synthesized. The synthesis of Zn_3P_2 nanobelts and Cd_3P_2 nanobelts with the VLS process is similar to that of the VS process except that In_2S_3 powder was added into the source materials. After reaction, wool-like products were also found deposited on the inner wall of the graphite cylinder where the temperature is about 900 °C. Indium is an efficient additive or catalyst for the growth of many kinds of 1D nanostructures. For example, Ren et al. reported the synthesis of various ZnO nanostructures in the presence of indium. During the reaction, InO_x vaporized first and formed the In_2O_3 nanowires, which act as the deposition sites for later ZnO growth. We also used indium to control the morphology of ZnO nanonails.[22]

Figure 7a is the SEM and TEM images of the obtained Zn_3P_2 nanobelts when In_2S_3 powders were added in the ZnS and Mn_3P_2 source materials, whereas the other conditions were kept unchanged. The obtained nanobelts have uniform diameters of ∼50 nm and lengths of several tens of micrometers. Contrary to the nanobelts synthesized with only ZnS and Mn_3P_2 as source materials, the tips of most of the nanobelts synthesized by utilizing In_2S_3 are capped with spherical particles as shown in the Figure 7a inset. EDS analysis reveals that the particles are composed of mainly In, and marginal Zn and S, indicating the formation of Zn_3P_2 nanobelts via an In-catalyzed VLS mechanism instead of the VS mechanism.

The microstructures of the synthesized Zn_3P_2 nanobelts were studied with the HRTEM technique. Figure 8a shows a TEM image of an individual Zn_3P_2 nanobelt, which has a uniform diameter of ∼50 nm along its whole length. The corresponding

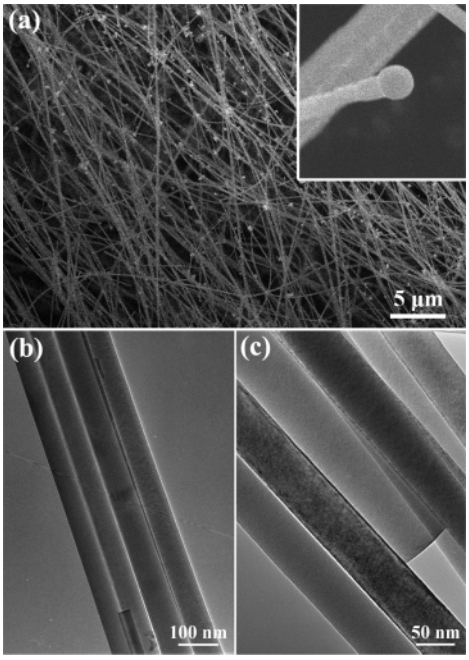

Figure 7. (a) SEM image of the synthesized Zn_3P_2 nanobelts with use of ZnS, Mn_3P_2, and In_2S_3 as the source materials. (b, c) TEM images of the synthesized Zn_3P_2 nanobelts.

SAED pattern shown in Figure 8b indicates its single crystalline nature. A TEM image of the nanobelt tip is shown in Figure 8c. A particle attached to the nanobelt is clearly seen, verifying the preferred VLS mechanism. Figure 8d demonstrates a HRTEM image of such VLS grown Zn_3P_2 nanobelts. The clearly resolved interplanar *d* spacing is 0.33 nm. This corresponds to the (202) lattice plane separation in tetragonal Zn_3P_2. The results indicate that the VLS grown Zn_3P_2 nanobelts are single crystals with the preferred growth directions perpendicular to the (101) planes, which is quite different from the VS grown Zn_3P_2 nanobelts. Several tens of VLS grown Zn_3P_2 nanobelts were checked, all displaying the same results. Thus, the present work also provides an efficient route for the synthesis of II_3-V_5 nanobelts with tunable growth directions. In the presence of indium, the Zn−In−P phase is formed at an early stage, which gives rise to a certain strain to change the surface free energy. The nucleation behavior of Zn_3P_2 at the solid−liquid interface is thus modified, which resulted in the formation of nanobelts having growth directions different from those of VS. In fact, tuning the growth directions of 1D nanostructures by changing experimental parameters, such as catalyst material, reaction temperature, additional promoters, and/or additives, has already been reported for many kinds of 1D nanostructures.[23]

A similar VLS process was also useful for the synthesis of Cd_3P_2 nanobelts. As shown in Figure 9a, the obtained nanobelts have diameters of about 120 nm. They are single crystals with the preferred growth directions perpendicular to the (101) planes, as shown in Figure 9b,c, similar to the VLS grown Zn_3P_2 nanobelts.

Cathodoluminescence (CL) properties of the synthesized nanobelts were also studied. Figure 10 shows the CL spectrum of the VS grown Zn_3P_2 nanobelts measured at about 20 K. A weak emission centered at about 785 nm was observed for the nanobelts. This value is comparable to that of bulk Zn_3P_2 crystals. No emission shift was observed since all the synthesized Zn_3P_2 nanobelts have diameters of about 100−200 nm and a wall thickness of about 40 nm. A similar result was obtained for the VLS grown Zn_3P_2 nanobelts. We also checked

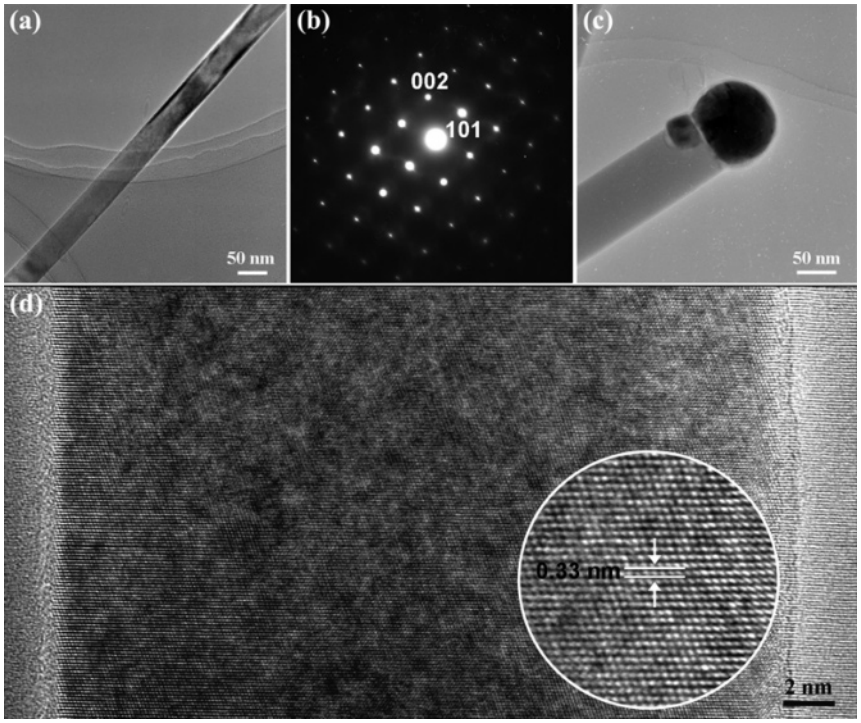

Figure 8. (a) TEM image and (b) its SAED pattern of a single Zn_3P_2 nanobelt. (c) TEM image of the tip of a Zn_3P_2 nanobelt. (d) HRTEM image of the Zn_3P_2 nanobelt synthesized via the VLS process.

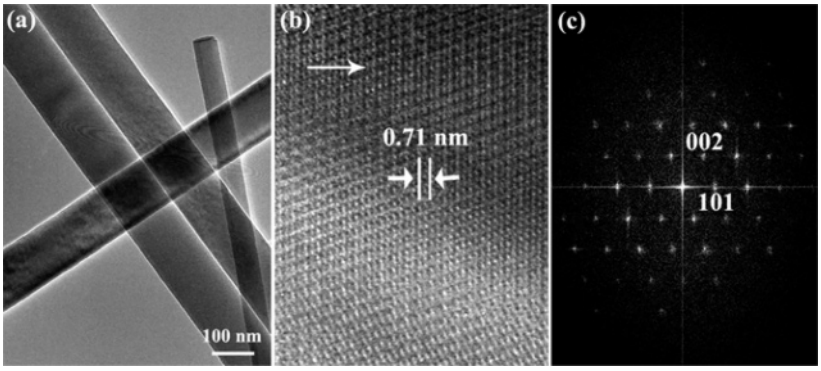

Figure 9. (a) TEM image of the VLS grown Cd_3P_2 nanobelts. (b, c) HRTEM image and its FFT image of a single Cd_3P_2 nanobelt.

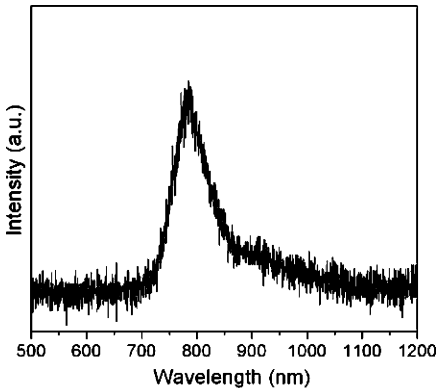

Figure 10. CL spectrum of the synthesized Zn_3P_2 nanobelts.

the CL properties of the synthesized Cd_3P_2 nanobelts. Unfortunately, no obvious emission was observed.

4. Conclusion

In conclusion, a simple thermal reaction process has been developed for the fabrication of high-quality Zn_3P_2 and Cd_3P_2 nanobelts on a large scale with use of ZnS and Mn_3P_2 as the source materials. The synthesized Zn_3P_2 nanobelts have diameters of about 100−200 nm and a wall thickness of about 40 nm while the Cd_3P_2 nanobelts have diameters of 100−500 nm, a thickness of ca. 70 nm, and lengths of hundreds of micrometers. Both kinds of nanobelts are single crystals with the preferred growth directions along the (010) crystallographic orientations without any sheathed materials. With the introduce of indium catalyst, nanobelts with different growth directions, perpendicular to the (101) planes, are fabricated. High-quality Zn_3P_2 and Cd_3P_2 nanobelts synthesized here may be valuable for the fabrication of a diverse range of functional semiconducting nanodevices. By a judicious choice of source materials, this method may be used for the fabrication of other II_3-V_2 nanobelts, such as Cd_3As_2, Zn_3As_2, etc.

References and Notes

(1) (a) Sun, S. H.; Murray, C. B.; Weller, D.; Folks, L.; Moser, A. *Science* **2000**, *287*, 1989. (b) Alivisatos, A. P. *Science* **1996**, *271*, 933. (c) Mann, S. *Nature* **1988**, *322*, 119.

(2) (a) Peng, X. G.; Manna, L.; Yang, W. D.; Wickham, J.; Scher, E.; Kadavanich, A.; Alivisatos, A. P. *Nature* **2000**, *404*, 59. (b) Mitchell, G. P.; Mirkin, C. A.; Letsinger, R. L. *J. Am. Chem. Soc.* **1999**, *121*, 8122. (c) Hu, J. T.; Odom, T. W.; Lieber, C. M. *Acc. Chem. Res.* **1999**, *32*, 425.

(3) (a) Lieber, C. M. *Solid State Commun.* **1998**, *107*, 106. (b) Duan, X. F.; Lieber, C. M. *Adv. Mater.* **2001**, *12*, 298. (c) Murray, C. B.; Norris, D. J.; Bawendi, M. G. *J. Am. Chem. Soc.* **1993**, *115*, 8706.

(4) (a) Dai, H. J.; Wong, E. W.; Lu, Y. Z.; Fan, S. S.; Lieber, C. M. *Nature* **1995**, *375*, 769. (b) Martin, C. R. *Science* **1994**, *266*, 1961.

(5) (a) Iijima, S. *Nature* **1991**, *354*, 56. (b) Tenne, R.; Margulis, L.; Genut, M.; Hodes, G. *Nature* **1992**, *360*, 444. (c) Feldman, Y.; Wasserman, E.; Srolovitz, D. J.; Tenne, R. *Science* **1995**, *267*, 222. (d) Chopra, N. G.; Luyken, R. J.; Cherrey, K.; Crespi, V. H.; Cohen, M. L.; Louie, S. G.; Zettl, A. *Science* **1995**, *269*, 966.

(6) (a) Morales, A. M.; Lieber, C. M. *Science* **1998**, *279*, 208. (b) Wang, D. W.; Dai, H. J. *Angew. Chem., Int. Ed.* **2002**, *41*, 4783. (c) Han, W. Q.; Fan, S. S.; Li, Q. Q.; Hu, Y. D. *Science* **1997**, *277*, 1287.

(7) (a) Goldberger, J.; He, R. R.; Zhang, Y. F.; Lee, S. K.; Yan, H.; Choi, H. J.; Yang, P. D. *Nature* **2003**, *422*, 599. (b) Hu, J. Q.; Bando, Y.; Zhan, J. H.; Golberg, D. *Angew. Chem., Int. Ed.* **2004**, *43*, 4606. (c) Hu, J. Q.; Bando, Y.; Zhan, J. H.; Zhi, C. Y.; Golberg, D. *Nano Lett.* **2006**, *6*, 1136.

(8) (a) Gates, B.; Yin, Y. D.; Xia, Y. N. *J. Am. Chem. Soc.* **2000**, *122*, 12582. (b) Pan, Z. W.; Dai, Z. R.; Wang, Z. L. *Science* **2001**, *291*, 1947. (c) Huang, M.; Mao, S.; Feick, H.; Yan, H.; Yu, Y.; Kind, H.; Weber, E.; Russo, R.; Yang, P. D. *Science* **2001**, *292*, 1897.

(9) (a) Wang, X.; Li, Y. D. *Angew. Chem., Int. Ed.* **2002**, *41*, 4790. (b) Li, Y. D.; Wang, J.; Deng, Z.; Wu, Y.; Sun, X.; Yu, D. P.; Yang, P. D. *J. Am. Chem. Soc.* **2001**, *123*, 9904.

(10) (a) Ye, C. H.; Meng, G. W.; Jiang, Z.; Wang, Y. H.; Wang, G.; Zhang, L. D. *J. Am. Chem. Soc.* **2002**, *124*, 15180. (b) Yang, J.; Liu, Y. C.; Lin, H. M.; Chen, C. C. *Adv. Mater.* **2004**, *16*, 713.

(11) (a) Kong, X. Y.; Ding, Y.; Yang, R. S.; Wang, Z. L. *Science* **2004**, *303*, 1348. (b) Gao, P. X.; Ding, Y.; Mai, W. J.; Hughes, W. L.; Lao, C.; Wang, Z. L. *Science* **2005**, *309*, 1700.

(12) (a) Zhang, H. F.; Wang, C. M.; Buck, E. C.; Wang, L. S. *Nano Lett.* **2003**, *3*, 577. (b) Shen, G. Z.; Bando, Y.; Zhi, C. Y.; Yuan, X. L.; Sekiguchi, T.; Golberg, D. *Appl. Phys. Lett.* **2006**, *88*, 243106. (c) Yuan, J. K.; Li, W. N.; Gomez, S.; Suib, S. L. *J. Am. Chem. Soc.* **2005**, *127*, 14184.

(13) (a) Liu, B.; Zeng, H. C. *J. Am. Chem. Soc.* **2003**, *125*, 4430. (b) Shen, G. Z.; Chen, D. *J. Am. Chem. Soc.* **2006**, *128*, 11762. (c) Lao, J. Y.; Wen, J. G.; Ren, Z. F. *Nano Lett.* **2002**, *2*, 1287. (d) Liu, B.; Zeng, H. C. *J. Am. Chem. Soc.* **2004**, *126*, 8124. (e) Lao, J. Y.; Huang, J. Y.; Wang, D. Z.; Ren, Z. F. *Nano Lett.* **2003**, *3*, 235.

(14) (a) Kar, S.; Chaudhuri, S. *J. Phys. Chem. B* **2005**, *109*, 3298. (b) Kar, S.; Pal, B. N.; Chaudhuri, S.; Chakravorty, D. *J. Phys. Chem. B* **2006**, *110*, 4605. (c) Patzke, G. R.; Krumeich, F.; Nesper, R. *Angew. Chem., Int. Ed.* **2002**, *41*, 2446. (d) Zhang, R. Q.; Lifshitz, Y.; Lee, S. T. *Adv. Mater.* **2003**, *15*, 635.

(15) (a) Ye, C. H.; Zhang, L. D.; Fang, X. S.; Wang, Y. H.; Yan, P.; Zhao, J. W. *Adv. Mater.* **2004**, *16*, 1019. (b) Chen, D.; Tang, K. B.; Liang, Z. H.; Liu, Y. K.; Zheng, H. G. *Nanotechnology* **2005**, *16*, 2619. (c) Liu, B.; Zeng, H. C. *J. Am. Chem. Soc.* **2004**, *126*, 16744.

(16) Madelung, O. *Data in Science and Technology*: *Semiconductors other Than Group IV Elements and III−V compounds*: Springer: Berlin, Germany, 1991.

(17) (a) Zdanowicz, W.; Zdanowicz, L. *Annu. Rev. Mater. Sci.* **1975**, *5*, 301. (b) Arushanov, E. K. *Prog. Cryst. Growth Charact.* **1980**, *3*, 211. (c) Lazarev, V. B.; Schevchenko, V. Y.; Greenberg, Y. H.; Sobolein, V. V. *II−V Semiconducting compounds*: Nauka: Moscow, Russia, 1978. (d) Bushan, M.; Catalano, A. *Appl. Phys. Lett.* **1981**, *38*, 39.

(18) (a) Green, M.; O'Brien, P. *Adv. Mater.* **1998**, *10*, 527. (b) Green, M.; O'Brien, P. *J. Mater. Chem.* **1999**, *9*, 243. (c) Green, M.; O'Brien, P. *Chem. Mater.* **2001**, *13*, 4500.

(19) (a) Weller, H.; Fojtik, A.; Henglein, A. *Chem. Phys. Lett.* **1985**, *117*, 485. (b) Goel, S. C.; Chang, M. Y.; Buhro, W. E. *J. Am. Chem. Soc.* **1990**, *112*, 5636.

(20) (a) Shen, G. Z.; Bando, Y.; Hu, J. Q.; Golberg, D. *Appl. Phys. Lett.* **2006**, *88*, 143105. (b) Shen, G. Z.; Bando, Y.; Ye, C. H.; Yuan, X. L.; Sekiguchi, T.; Golberg, D. *Angew. Chem., Int. Ed.* **2006**, *45*, 7568.

(21) (a) Wagner, R. S.; Ellis, W. C. *Appl. Phys. Lett.* **1964**, *4*, 89. (b) Sears, G. W. *Acta Metall.* **1956**, *3*, 268.

(22) (a) Shen, G. Z.; Bando, Y.; Chen, D.; Liu, B. D.; Zhi, C. Y.; Golberg, D. *J. Phys. Chem. B* **2006**, *110*, 3973. (b) Shen, G. Z.; Cho, J. H.; Lee, C. J. *Chem. Phys. Lett.* **2005**, *401*, 414.

(23) (a) Kuykendall, T.; Pauzauskie, P.; Lee, S.; Zhang, Y.; Goldberger, J.; Yang, P. D. *Nano lett.* **2003**, *3*, 1063. (b) Wang, Z. L. *Adv. Mater.* **2003**, *15*, 432. (c) Ding, Y.; Gao, P. X.; Wang, Z. L. *J. Am. Chem. Soc.* **2004**, *126*, 2066. (d) Fan, H. J.; Fuhrmann, B.; Scholz, R.; Himcinschi, C.; Berger, A.; Leipner, H.; Dadgar, A.; Krost, A.; Christiansen, S.; Gosele, U.; Zacharias, M. *Nanotechnology* **2006**, *17*, S231.